

Dynamic localization of two-dimensional electrons at mesoscopic length scales

A. Ghosh, M. Pepper, H. E. Beere, and D. A. Ritchie

Cavendish Laboratory, University of Cambridge, Madingley Road, Cambridge CB3 0HE, United Kingdom

(Received 16 September 2004; published 17 December 2004)

We have investigated the local magnetotransport in high quality two-dimensional electron systems at low carrier densities. The positive magnetoresistance in perpendicular magnetic field in the strongly insulating regime has been measured to evaluate the spatial concentration of electron trap sites within a mesoscopic region of the samples. A simultaneous measurement of the electron density within the same region shows an unexpected correspondence between the density of electrons in the metallic regime and that of the localizing sites in the insulating phase. We have shown this to imply a self-localized many-body ground state in the interacting regime, stabilized by optimal disorder.

DOI: 10.1103/PhysRevB.70.233309

PACS number(s): 73.21.-b, 73.20.Qt

The nature of localization of electrons in low dimensional systems is a matter of continuing debate. In the nonpercolative models, short-range disorder gives rise to “trap” sites close to the Fermi energy (E_F), where the electronic states can be localized.^{1,2} These sites, conventionally assumed to be impurity bound and randomly distributed in space, play a central role in the hopping-type transport at low temperatures. When the Coulomb interaction is taken into account perturbatively, the nature of hopping transport is significantly modified, but the origin and nature of the trap sites are assumed to remain unchanged.² Recent theoretical investigations have, however, indicated that beyond the perturbative regime, Coulomb interaction may delocalize the charge carriers from the impurity-bound sites to form a more uniform spatial distribution,³ and eventually self-localize in some form of charge-density waves as the carrier-density is lowered.⁴ The concentration and distribution of the localizing sites in such a case would be independent of the spatial locations of impurities. Experimentally, local compressibility studies remain inconclusive regarding any such impurity-independent localization.^{5,6} Here, we have carried out a direct evaluation of the density of the trap sites (n_L) within mesoscopic regions of high quality two-dimensional electron systems (2DES's) in the strongly interacting regime. Unexpectedly, over a limited range of electron density (n_s) (and background disorder), we find n_L to be gate voltage (V_g) dependent, and correspond to n_s itself, irrespective of background disorder. We propose that this is an evidence of a self-localized insulating phase, where disorder plays only a stabilizing role.

In disordered 2DES's, the strongly localized regime is identified by a longitudinal resistivity $\rho \gg h/e^2$, and an activated (nearest-neighbor) hopping or a variable-range hopping transport, where $\rho(T) \sim \exp(T_0/T)^p$, T_0 and p being the relevant energy scale and hopping exponent, respectively. In a weak magnetic field (B), applied perpendicular to the plane of the 2DES, the asymptotic behavior of the electronic wave function of an isolated impurity-bound state changes to $\psi(r) \sim \exp(-r/\xi - r^3\xi/24\lambda^4)$, where ξ is the localization length and $\lambda = \sqrt{\hbar/eB} \gg \xi$.^{7,8} The B -induced compression of the wave function leads to a strong positive magnetoresistance (MR), which is expressed analytically as $\rho(T, B)$

$= \rho(T, B=0) \exp(\alpha B^2)$. An expression for α has been derived from the shift in percolation threshold, which in the limit of narrow bandwidth can be expressed as⁹

$$\alpha \approx A_L \frac{e^2 \xi}{\hbar^2 n_L^{3/2}}, \quad (1)$$

where A_L is a model-dependent constant of order unity, whose precise value will be discussed later. Equation (1) provides a mechanism of estimating n_L from the weak-field MR in strongly localized systems, and has been used in the context of hopping transport in the impurity band of δ -doped GaAs.¹⁰

Mesoscopic segments of high-mobility Si δ -doped (doping density $n_\delta = 2.5 \times 10^{12} \text{ cm}^{-2}$) GaAs/AlGaAs heterostructures were created by the intersection of a narrow bridge in the mesa (width: W) and a transverse Au/NiCr metallic gate (width: L) [Fig. 1(a)]. The n_s within the active region depends on the V_g through the specific capacitance C_0 . Within the simple capacitor model, $C_0 \approx \epsilon_0 \epsilon_r / ed_s$, where d_s is the depth of the 2DES from the surface. The background disorder, and hence the electron mobility μ , were varied by changing the spacer thickness (δ_{sp}) between the dopant layer and the GaAs/AlGaAs interface. For this experiment we have chosen mesoscopic samples from two heterostructures (referred to as A07 and A78), which differ in δ_{sp} and d_s , but identical in all other structural and geometrical aspects. The relevant parameters are given in Table I. In order to minimize the effect of contact and series resistances, the electrical measurements were carried out only in four-probe geometry with a low-frequency ($\sim 7.2 \text{ Hz}$) ac excitation current of $\sim 0.01 - 0.1 \text{ nA}$. The maximum measured resistance was limited to $\sim 1.5 \text{ M}\Omega$ to avoid any systematic error arising from stray capacitances.

The first part of the experiment calibrates the V_g dependence of n_s in the metallic regime when $\rho \ll h/e^2$ and quantum Hall-based methods are applicable. We have used a technique based on the reflection of edge states, which was originally developed to study backscattering of edge states by well-defined potential barriers.¹¹ The technique is schematically represented in Fig. 1(a). Briefly, when the perpendicular B corresponds to ν_0 edge channels in the ungated part

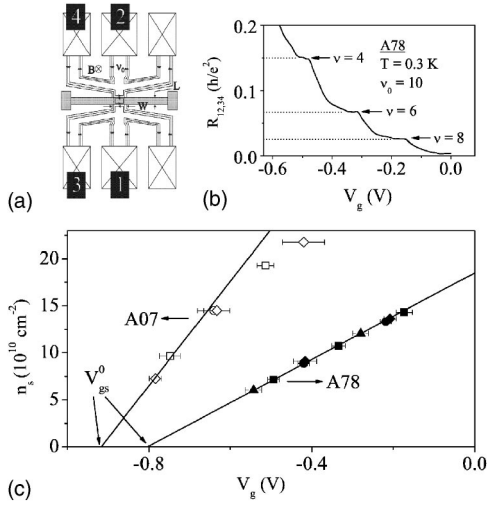


FIG. 1. (a) A schematic of the device structure. Contacts 1 and 2 are for current probes, while 3 and 4 are used for voltage probes. (b) Illustration of gate voltage (V_g) dependence of the four-probe resistance $R_{12,34}$ at a constant magnetic field ($B=0.742$ T) corresponding to an integral filling factor $\nu_0 (=10)$ in sample A78. The dashed lines are the expected values of $R_{12,34}$ at different filling factors ν within the gated region (see text). (c) $n_s = eB\nu/h$, at values of V_g 's corresponding to the center of the plateaus in $R_{12,34}$. The horizontal error bars represent the width of the plateaus in V_g . The solid lines are fits to the linear part of the data. For both samples, different symbols correspond to different integral value of ν_0 at which $R_{12,34}-V_g$ sweeps were recorded.

of the Hall bar, a negative V_g will cause $\nu_0 - \nu$ of the channels to get reflected at the gate, where ν is the filling factor within the active region. As a function of V_g , this leads to plateaus in the four-probe resistance ($R_{12,34}$) at $R_{12,34} = (h/e^2)(1/\nu - 1/\nu_0)$, when the contacts (1–4) in Fig. 1(a) are close to ideal with no reflection and perfect transmission. This is illustrated in Fig. 1(b), where the V_g -dependence of $R_{12,34}$ is measured in sample A78 at a constant B corresponding to $\nu_0 = 10$. Three plateaus corresponding to $\nu = 8, 6,$ and 4 appear nearly exactly at the theoretically expected values (horizontal dashed lines). The V_g at the center of these plateaus then corresponds to an electron density of $n_s = eB\nu/h$, while the width of the plateau represents the maximum uncertainty. For both samples, we have repeated this measurement for different values of ν_0 (within spin degeneracy).

Figure 1(c) shows n_s as a function of V_g for samples A07 (empty symbols) and A78 (filled symbols). At a sufficiently negative V_g both samples display the expected linear dependence of n_s on V_g . In A07, the deviation from linearity at higher V_g can be explained from screening of V_g by accumu-

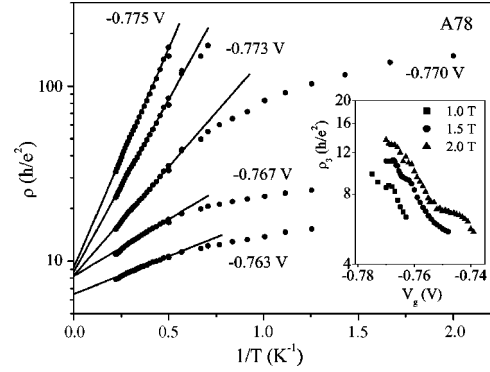


FIG. 2. Temperature dependence of resistivity ρ in A78 for different values of gate voltage (V_g) recorded at $B=1$ T. Inset: gate-voltage dependence of the pre-exponential factor ρ_3 at three magnetic fields.

lation of carriers in the dopant layer.¹² When the linear part was fitted with $n_s = C_s(V_g - V_{gs}^0)$, the slope C_s was found to be $\approx 55.5 \times 10^{10} \text{ cm}^{-2} \text{ V}^{-1}$ for A07 and $\approx 23.0 \times 10^{10} \text{ cm}^{-2} \text{ V}^{-1}$ for A78, agreeing satisfactorily with the corresponding values of C_0 . The intercept V_{gs}^0 was found to be $V_{gs}^0 = -0.917 \pm 0.004$ V and -0.804 ± 0.002 V for A07 and A78, respectively.

We now consider the strongly localized regime, where $\rho \gg h/e^2$. Both systems displayed the “metal”-insulator transition at a critical resistivity $\rho_c \sim 0.1 - 0.2 \times h/e^2$. To ensure strong localization and consistency in the subsequent analysis, we have limited ourselves to the regime of V_g for which $\rho \geq 2h/e^2$ at $T=0.3$ K and $B=0$ T, which exceeds ρ_c by more than an order of magnitude. As shown in the insets of Fig. 3, this regime corresponds to $V_g \leq -0.86$ V for A07 and $V_g \leq -0.74$ V for A78. By extrapolating the $n_s - V_g$ calibration, we find the Coulomb interaction in this regime to be strong, with the interaction parameter $r_s (= 1/a_B^* \sqrt{\pi n_s})$ varying over $r_s \sim 2.8 - 5.2$ in A07 and $\sim 4.4 - 7.0$ in A78 (a_B^* is the effective 3D Bohr radius).

In order to investigate the nature of localized-state transport, we have measured the T dependence of ρ at various V_g . This is illustrated in Fig. 2 for A78 at $B=1$ T. At higher T (≥ 1.8 K), the activated behavior of $\rho = \rho_3 \exp(\epsilon_3/k_B T)$, clearly indicates nearest-neighbor hopping as the energy term ($\epsilon_3/k_B T$) becomes dominant over the site term (r/ξ).¹⁰ This would explain the weakening T dependence of ρ with decreasing temperature as the onset of variable range hopping. The hopping mechanism of transport is also confirmed by the strong enhancement of the pre-exponential factor ρ_3 with decreasing V_g .⁸ This is shown in the inset of Fig. 2 for three different magnetic fields. Furthermore, $\rho_3 \gg \rho_c$ at all V_g ,

TABLE I. Relevant parameters of the samples used. $\mu(0)$ and $n_s(0)$ are as-grown mobility and electron density, respectively.

Sample	$\mu(0)$ $\text{cm}^2/\text{V s}$	$n_s(0)$ cm^{-2}	δ_{sp} nm	d_s nm	$L \times W$ $\mu\text{m} \times \mu\text{m}$	C_0 $\text{cm}^{-2} \text{V}^{-1}$
A07	0.6×10^6	2.9×10^{11}	20	120	2×8	57×10^{10}
A78	1.8×10^6	2.1×10^{11}	40	290	2×8	24×10^{10}

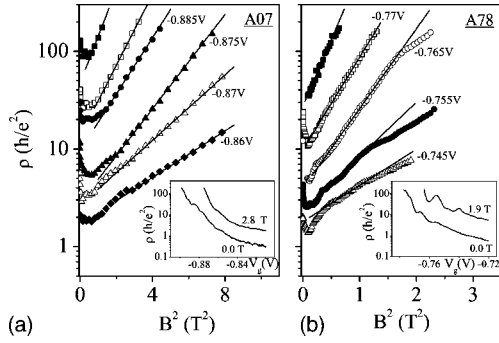


FIG. 3. Dependence of resistivity ρ on B^2 for different values of gate voltage (V_g) recorded at $T=0.3$ K. Inset: V_g dependence of ρ at zero and finite B . (a) sample A07, and (b) sample A78.

which eliminates excitation to the mobility edge as the origin of the activated behavior.

The MR at $T \approx 0.3$ K is shown in Fig. 3 for A07 and A78. Increasing B from zero initially results in some negative MR in both samples, followed by an exponential rise in $\rho(B)$ at higher B . From Fig. 3, $\ln \rho$ varies linearly with B^2 over a field range of $1.2 \leq B \leq 3$ T for A07 and $0.5 \leq B \leq 1.3$ T for A78. The lower limit of this linear dependence is determined by the extent of negative MR, which arises from an interference among the hopping paths.¹³ The upper cutoff in B probably arises from the strong-field condition $r \ll \lambda^2/\xi$ for the asymptotic form of the wave function $\psi(r)$.^{7,8} The slope α of the $\ln \rho - B^2$ traces was found to decrease with increasing V_g in both samples, being independent of temperature up to $T \approx 2$ K for a fixed V_g . This is illustrated for A78 at $V_g = -0.770$, -0.760 , and -0.750 V in the inset of Fig. 5.

We now discuss the implications of the decreasing trend in α with increasing V_g . As shown in Fig. 4, α decreases over a factor of ~ 5 in both samples within the strongly localized regime. We first consider the variable range hopping at weak B in an impurity band with bandwidth $\gg k_B T$, where it has been shown that $\ln \rho(B)/\rho(0) = c_p (T_0/T)^{3p} \xi^4/\lambda^4$, c_p being a

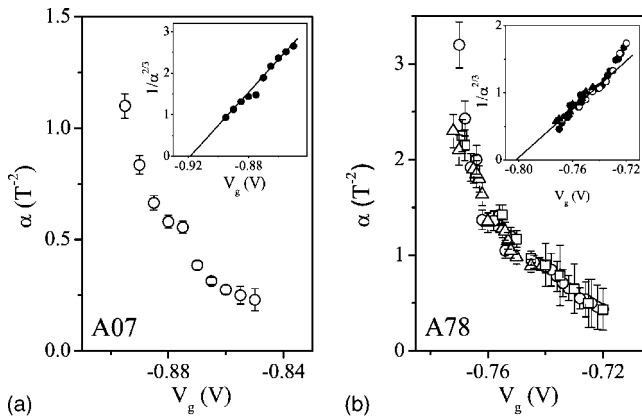


FIG. 4. Gate voltage (V_g) dependence of the slope (α) of the linear region of $\ln(\rho) - B^2$ data shown in Fig. 3. The data were obtained at $T=0.3$ K. The fit uncertainty increases, and hence the error bar on α , as ρ decreases to $\sim 2h/e^2$. (a) sample A07, and (b) sample A78. Inset (a), (b): dependence of $\alpha^{-2/3}$ on V_g . The solid lines depict the approximately linear behavior.

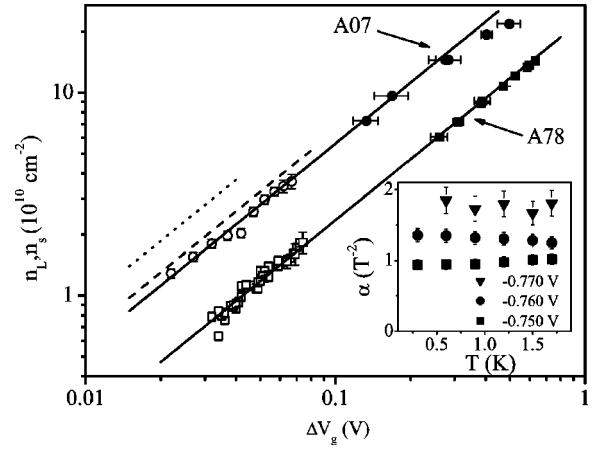


FIG. 5. Correspondence between n_L and n_s . For clarity, n_L , $n_s - \Delta V_g$ are plotted in log-log scale, where $\Delta V_g = V_g - V_{gL}^0$ for n_L (empty symbols) and $V_g - V_{gs}^0$ for n_s (filled symbols). For A07, the dashed and dotted lines represent estimates of n_L assuming $A_L = 0.083$ and 0.143 , respectively. Inset: temperature dependence α at three gate voltages for A78.

numerical constant.⁷ This would lead to $\alpha \sim \xi^{5/2}/T^{3/2}$ for $p = 1/2$ (Efros-Shklovskii hopping) or $\alpha \sim \xi^2/T$ for $p = 1/3$ (Mott hopping). Qualitatively, such T and ξ dependence of α has been observed for hopping in the Na^+ impurity band of Si-metal-oxide-semiconductor field-effect transistor (MOSFET's), where α was found to increase as the Fermi energy was swept towards band half-filling.¹⁴ In our case, however, this scenario fails on two accounts: (i) α is found to be T independent (inset of Fig. 5), and (ii) α is expected to increase with increasing V_g . This is because as the system is driven more metallic, effective screening of the impurity potentials would result in rapidly increasing ξ , and hence α .

The T independence of α can be explained by assuming hopping transport within a narrow (but finite) impurity band, where α is given by Eq. (1). However, a physically reasonable explanation for the experimentally observed trend of α with V_g invariably requires, (i) ξ to be only weakly dependent on V_g and, (ii) a V_g -dependent n_L , which increases with increasing V_g . The latter aspect implies that the positions of available trap sites for the hopping electrons are determined by the distribution of the other localized electrons in the system, rather than the background disorder. Recent imaging of the localized states in the quantum Hall regime has also indicated a dynamic pattern in the localized charge density evolving continuously with V_g .⁵ In our case, however, we note two additional aspects of the data which indicate that n_L is strongly associated to the electron density n_s itself: (i) As shown in the insets of Figs. 4(a) and 4(b), $1/\alpha^{2/3}$ shows a near-linear dependence on V_g for both samples. Moreover, an extrapolation of this dependence reveals intercepts $V_{gL}^0 = -0.918 \pm 0.004$ V for A07 and -0.806 ± 0.006 V for A78, which agree very well with the corresponding values of V_{gs}^0 within the experimental uncertainty. (ii) The absolute magnitude of α is about a factor of ~ 2 larger in A78, implying a smaller n_L . Correspondingly, extrapolation of the $n_s - V_g$ calibration shows that A78 indeed localizes at a smaller value of n_s than that for A07.

Estimation of the absolute magnitude of n_L from Eq. (1) requires an estimate of A_L and ξ . If the system consists of only two isolated localized states, one obtains A_L simply from the overlap integral as $A_L = 1/12 \approx 0.083$.¹⁵ However, in the hopping regime there is a large number of states, and the relation $A_L = (N_c/\pi)^{3/2}/12$ can be obtained following Nguen's analysis of the B -induced shift in percolation threshold.⁹ Here N_c is the dimensionality-dependent number of bonds per site in the random resistor network. $N_c = 4.5$ or 2.7 , for zero or finite width of the impurity band with respect to $k_B T$.^{14,16} This gives $A_L \approx 0.143$ and 0.0664 , respectively. Note that all the estimates of A_L are within a factor of ~ 2 , and hence only have a fine-tuning effect on the absolute magnitude of n_L . In the strongly localized regime where $\rho \gg \rho_c$, following Ref. 10, we assume $\xi \sim a_B^* \approx 10.5$ nm. As shown in Fig. 5, using $A_L = 0.0664$ and $\xi = 10.5$ nm, we find an excellent correspondence between n_L and n_s as a function of the gate voltage in both samples (solid line). The dashed and the dotted lines depict the magnitude of n_L using $A_L = 0.083$ and 0.143 , respectively. This agreement also confirms the validity of Eq. (1) in our analysis.

The correspondence between n_L and n_s implies that on the average every electron in the system is associated with one trap site. A possible way to realize this would be if the electrons are self-localized in an ordered or disordered array in space. In the absence of disorder, strong Coulomb interaction is known to give rise to several possibilities that include Wigner crystals, bubble or striped phases.¹⁷ It is suggested that the role of disorder, which in our case arises from the Coulomb potential of the dopants, in stabilizing such phases

is critical, providing an overall pinning and a positive background. Recent numerical simulations have indicated the possibility of stabilizing a Wigner-like distribution of electrons at relatively high electron densities ($r_s \sim 7.5$) in the presence of optimal disorder.⁴ The quantitative effect of disorder on the relevant energy scales of transport is, however, unclear. For A78, the activation energy (ϵ_3) for the nearest-neighbor hopping was found to be only ~ 0.1 – 0.5 meV (Fig. 2). This is nearly an order of magnitude smaller than the (unscreened) pinning potential ($\sim e^2/4\pi\epsilon_0\epsilon_r\delta_{sp} \approx 3$ meV) one would expect if the localized states arise from the dipole interaction between a hole in the GaAs/AlGaAs interface and an acceptor state in the δ -doped layer. It should, however, be emphasized that, we cannot, at present, make a definite comment on any specific spatial order in the distribution of the localized states. This would require further understanding of the geometrical parameters, in particular A_L , which is presently under investigation.

In conclusion, magnetotransport in the strongly localized, low-density regime of high quality 2D electron systems provides evidence of a dynamic, gate voltage-dependent distribution of localizing sites. Over a mesoscopic region of the 2D systems, the spatial density of these sites was found to agree with the estimated density of electrons at the same gate voltage, independent of background disorder. This correspondence indicates an unusual insulating ground state in two dimensions where the carriers are self-localized under the influence of strong electron-electron interaction.

We thank EPSRC for support. A.G. wishes to thank Igor Aleiner for a fruitful discussion.

-
- ¹N. F. Mott and E. A. Davis, in *Electronic Processes in Non-Crystalline Materials* (Clarendon Press, Oxford, 1979); T. Ando, A. B. Fowler, and F. Stern, *Rev. Mod. Phys.* **54**, 437 (1982); B. L. Altshuler, D. L. Maslov, and V. P. Pudalov, *Physica E (Amsterdam)* **9**, 209 (2001).
- ²A. L. Efros and B. I. Shklovskii, *J. Phys. C* **8**, L49 (1975).
- ³D. L. Shepelyansky, *Phys. Rev. Lett.* **73**, 2607 (1994); J. Shi and X. C. Xie, *ibid.* **88**, 086401 (2002).
- ⁴S. T. Chui and B. Tanatar, *Phys. Rev. Lett.* **74**, 458 (1995).
- ⁵N. B. Zhitenev *et al.*, *Nature (London)* **404**, 473 (2000).
- ⁶S. Ilani, A. Yacoby, D. Mahalu, and H. Shtrikman, *Science* **292**, 1354 (2001).
- ⁷B. I. Shklovskii, *Fiz. Tekh. Poluprovodn. (S.-Peterburg)* **17**, 2055 (1983) [*Sov. Phys. Semicond.* **17**, 1311 (1983)].
- ⁸B. I. Shklovskii and A. L. Efros, in *Electronic Properties of Doped Semiconductors*, Springer Series in Solid-State Sciences No. 45 (Springer, Berlin, 1984).
- ⁹V. L. Nguen, *Fiz. Tekh. Poluprovodn. (S.-Peterburg)* **18**, 335 (1984) [*Sov. Phys. Semicond.* **18**, 207 (1984)].
- ¹⁰Q. Y. Ye, B. I. Shklovskii, A. Zrenner, F. Koch, and K. Ploog, *Phys. Rev. B* **41**, 8477 (1990).
- ¹¹R. J. Haug, A. H. MacDonald, P. Streda, and K. von Klitzing, *Phys. Rev. Lett.* **61**, 2797 (1988); S. Washburn, A. B. Fowler, H. Schmid, and D. Kern, *ibid.* **61**, 2801 (1988).
- ¹²K. Hirakawa, H. Sakaki, and J. Yoshino, *Appl. Phys. Lett.* **45**, 253 (1984).
- ¹³W. Schirmacher, *Phys. Rev. B* **41**, 2461 (1990); V. L. Nguen, B. Z. Spivak, and B. I. Shklovskii, *Zh. Eksp. Teor. Fiz.* **89**, 1770 (1985) [*Sov. Phys. JETP* **62**, 1021 (1986)].
- ¹⁴G. Timp and A. B. Fowler, *Phys. Rev. B* **33**, 4392 (1986).
- ¹⁵A. K. Savchenko, V. V. Kuznetsov, A. Woolfe, D. R. Mace, M. Pepper, P. A. Ritchie, and G. A. C. Jones, *Phys. Rev. B* **52**, R17 021 (1995).
- ¹⁶P. N. Butcher and K. J. Hayden, *Philos. Mag.* **36**, 657 (1977).
- ¹⁷B. Tanatar and D. M. Ceperley, *Phys. Rev. B* **39**, 5005 (1989); A. A. Koulakov, M. M. Fogler, and B. I. Shklovskii, *Phys. Rev. Lett.* **76**, 499 (1996).